

Response to Anonymous Referee #2

Authors' responses to reviewer comments appear in blue text. Line numbers referenced in the authors' responses refer to the revised document. Figures with Arabic numerals (e.g., Figure 10) correspond to the revised manuscript, Figures with roman numerals (e.g., Figure iv) only appear on the response to reviewer's comments.

The objective of the article is to investigate the mechanisms driving the development of the wind speed deceleration in front of wind farms responsible for the global blockage effect. To achieve this, the authors perform Large Eddy Simulations using WRF-LES. They compare simulations of two different atmospheric stability regimes (moderately stable and weakly stable) each with the actuator disk representation of a single turbine or a 10 x 4 turbines wind farm (NREL 5 MW).

The assessment of the physical effects driving global blockage is performed analyzing the different contributions to the steady state integral momentum equation for the u – velocity where the Coriolis force and turbulence contributions are neglected. A vertical momentum advection is identified as the main cause of global blockage.

The paper contributes to the currently increasing number of numerical investigations of the global blockage effect. Even though the findings that the vertical advection of momentum out of the farm inflow is correlated to global blockage (Strickland and Stevens, 2022), as well as the dependency of global blockage on atmospheric stability (Schneemann et al. 2021) is not new itself, the approach to separate the different contributions causing the flow deficit upstream a wind farm is novel and interesting. However, in the current draft the manuscript lacks a clear description of the interesting findings, compromising the achievement of the paper's objective. The paper is generally well written but needs corrections and clarifications detailed below. Further, a revised manuscript should better follow a storyline. The Figures are mainly clear and support the results, some changes are suggested in the following. We recommend to publish the paper after our major concerns and questions are addressed.

Scientific comments

On the presentation of the physical mechanisms of global blockage

The paper's objective is to clarify the fundamental physics of Global Blockage. However, the main findings are not highlighted well enough, and the argumentation towards the main results is hard to follow.

The different strengths in blockage comparing single turbine and wind farm resulting from different amounts of the flow being advected upwards (i.e. different vertical momentum transport), is one of the main findings of the paper, and it should be made clearer. The authors could e.g. display the different vertical wind speeds in front of the single turbine and the wind farm in a single plot.

We appreciate your suggestion. We now include this figure in the manuscript. Note that we only show the vertical velocity for the upper half of the turbine rotor layer because the vertical velocity can be negative at the bottom of the turbine rotor layer (Figure i).

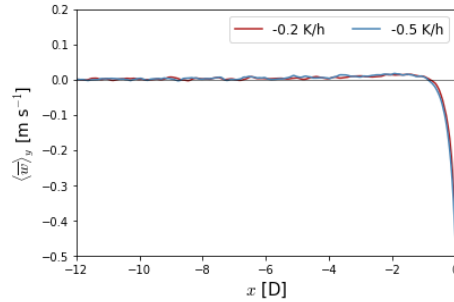


Figure i: Time-averaged vertical velocity at the bottom ($z = 27 \text{ m}$) of the turbine rotor layer for each atmospheric condition. The vertical velocity is averaged in the y -direction over the span of the wind plant.

We now include the vertical velocity upstream of a front-row turbine in the middle of the wind plant and of a stand-alone turbine as follows:

Line 309: “Therefore, differences in vertical transport of horizontal momentum between a stand-alone turbine and a turbine in the wind plant are entirely due to the vertical velocity that forms upstream of the turbine array (Figure 21). For the wind plant, the secondary flow (i.e., net upwards w -velocity) extends farther upstream than for a stand-alone turbine (Figure 21).”

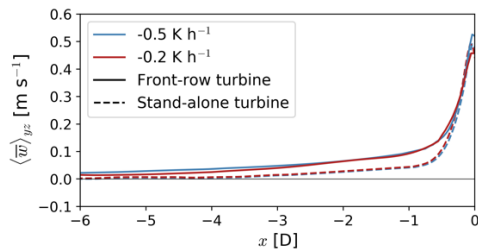


Figure 21: Streamwise evolution of the vertical velocity upstream of a stand-alone and front-row turbine in middle of the wind plant. The vertical velocity is averaged in the y -direction over the rotor diameter and in the z -direction over the top half of the rotor layer.

Another important finding is that the horizontal pressure gradient upstream of a turbine in isolation and a turbine in the first row of the farm is substantially equal. However, these results are very counterintuitive. In internal tests, the horizontal pressure gradient has been observed to increase dramatically between a turbine in isolation and a turbine at the first row of a farm. Could the authors explain this discrepancy? Could the authors confirm that the pressure gradient force for the front-row turbine in Figure 15a is normalized with the horizontal momentum advected only through the surface S_x of Figure 10c, instead of 10b? Please distinguish the variables for both S_x used.

We can confirm that the pressure gradient force is being normalized using the appropriate momentum flux at the inflow of the control volume. Given that there is no literature comparing the pressure gradient force for a wind plant and a single turbine, we cannot provide a definitive explanation for this discrepancy. When we evaluate the pressure gradient in the original numerical grid (without interpolation to the common $dx = 15 \text{ m}$ grid that is used in the control volume analysis), we clearly see that the pressure gradient upstream and downstream of a front-row turbine in the wind plant and a stand-alone turbine is almost perfectly overlapping (Figure ii).

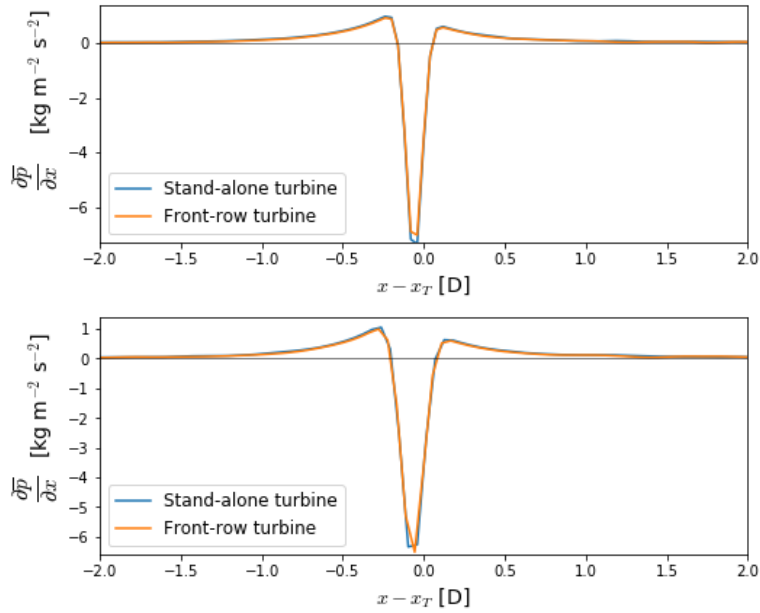


Figure ii: Pressure gradient in dimensional form for the moderate (top) and weak (bottom) stability cases within the turbine rotor layer.

We add clarification in our analysis to highlight that this behavior is observed in our simulations specifically and propose this as an avenue of future research:

Line 284: “The pressure gradient upstream of a single front-row turbine in the wind plant is virtually the same as the pressure gradient force for a stand-alone turbine for both atmospheric conditions in our simulations (Figure 17).”

Line 404: “In addition, more research is needed to further validate the forcing mechanisms driving blockage for a front-row turbine in the wind plant and a stand-alone turbine for a wide range of atmospheric conditions.”

We also modify Figure 11 and add clarification to its caption, and modify the captions of Figures 16,19 accordingly to distinguish between the different control volumes in our analysis.

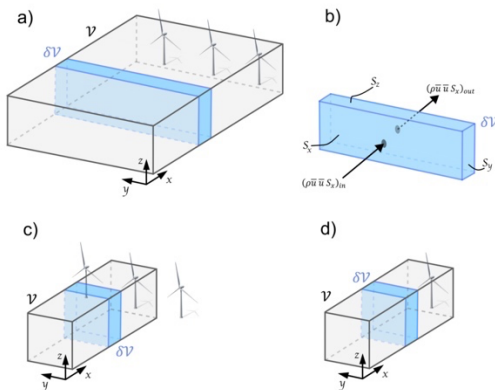


Figure 11: Illustration of the region considered in the analysis of the momentum balance along the x-direction for the whole wind plant (a), a single turbine in the front row of the wind plant (c) and stand-alone turbine (d). The integral momentum equation is evaluated on differential control volumes δV along the streamwise direction upstream of the turbines (b). Each control volume is bounded vertically by the top ($z = 153$ m) and bottom ($z = 27$ m) of the turbine rotor layer. Horizontally in the y-direction, the control volume spans the region upstream of the wind plant (from $y = 1953$ m to $y = 5922$ m). For the single and stand-alone turbine (c,d), the control volume is bounded in the y-direction by the rotor diameter. Each differential control volume is 15 m long in the x-direction. The area of each control surface S_i is illustrated in the differential control volume δV in Panel (b).

Figure 17,20: ... In panel (a), the integral momentum equation is evaluated on differential control volumes as shown in Figure 11c for a single turbine in the middle of the wind plant and as shown in Figure 11d for a stand-alone turbine. In panel (b), the integral momentum equation is evaluated on the control volume V shown in Figures 11c,d for a single turbine in the middle of the wind plant and for a stand-alone turbine. The pressure gradient force is normalized using the u-momentum flux at the inflow of the control volume V in Figures 11c,d far upstream $\rho \bar{u}_\infty \bar{u}_\infty S_x$ for the respective stability case.

Furthermore, as the horizontal pressure gradient does not change across all the studied cases, the authors postulate that what drives the changes in the vertical momentum advection is a vertical pressure gradient developing upstream of the farm. This vertical pressure gradient seems then to be identified as the main mechanism causing global blockage. Unfortunately, most of the very little discussion on it is relegated to the Appendix. The authors should consider introducing the plots for the integral momentum balance in the vertical direction in the body of the paper and expand the discussion on the vertical pressure gradient.

Thank you for highlighting this point because it is important for us to clarify. We do not state that the changes in vertical transport of u-momentum are mainly caused by changes in the vertical pressure gradient. Rather, we identify that the differences in vertical advection of horizontal momentum between both atmospheric conditions are primarily due to differences in vertical shear of the vertical velocity. We added clarification in the manuscript as follows:

Line 297: “The vertical velocity advects horizontal momentum out of the turbine rotor layer (Figure 19). Vertical advection of horizontal momentum is 20% larger in the moderate stability case compared to the weak stability upstream of the first turbine row (Figure 19b). Larger vertical shear of the horizontal velocity in the moderate stability case compared to the weak stability case is the primary cause for the increased vertical advection of horizontal momentum. Shear $\left(\frac{\Delta \bar{u}}{\Delta z} = \frac{\bar{u}_t - \bar{u}_b}{D}\right)$ between the bottom \bar{u}_b and top \bar{u}_t of the turbine rotor layer is 43.6% larger in the -0.5 K/h simulation compared to the -0.2 K/h simulation. Similarly, the vertical velocity in the turbine rotor layer is 20% larger in the moderate stability case than in the weak stability case between $x = -6D$ and $x = 0D$. The vertical velocity is expected to be larger in the moderate stability case because, as shown in Figure 18, the streamwise slowdown of the flow is transformed almost entirely into vertical motions. As a result, advection of horizontal momentum by the vertical velocity $\Delta(\rho \bar{u} \bar{w} S_z) = \rho S_z (\bar{u}_t \bar{w}_t - \bar{u}_b \bar{w}_b)$ is amplified.”

We also replace “vertical momentum transport” with “vertical transport of horizontal momentum” throughout the text. As an example, line 309 now reads: “Vertical advection of horizontal momentum is amplified for a wind plant compared to a stand-alone turbine (Figure 20). For a

given atmospheric condition, vertical shear of the horizontal velocity remains unchanged between the stand-alone turbine and wind plant simulations. Therefore, differences in vertical transport of horizontal momentum between a stand-alone turbine and a turbine in the wind plant are entirely due to the vertical velocity that forms upstream of the turbine array (Figure 21)."

Further analysis should also be performed to make the point of the authors stronger. As done for the horizontal momentum, also the vertical momentum balance should be compared between the wind farm and the single wind turbine cases. The claim of the authors could be supported by demonstrating that the vertical pressure gradient increases in the wind farm case, in the same order as the blockage increases.

Please see comment above, where we clarify that the primary cause for an increase in vertical advection of horizontal momentum is larger shear of the vertical velocity ($\frac{\Delta \bar{u}}{\Delta z}$) within the turbine rotor layer.

On gravity waves:

The authors write that gravity waves did not form in the weak free-atmosphere stratification simulation of Wu and Porté-Agel (2017) in Line 40-41. This statement might be misleading and it should be revised. In fact, Wu and Porté-Agel did not observe upstream propagating gravity waves in their simulation with a weak stratification in the free atmosphere. Wu and Porté-Agel (2017) differentiate between subcritical and supercritical flows. In subcritical flow gravity waves can move upstream, in supercritical flows they can't. Wu and Porté-Agel (2017) do not state that there are no gravity waves in case of the supercritical flow. My suggestion is to apply the theory presented in Wu and Porté-Agel (2017) in order to determine whether the cases shown by the authors are cases of supercritical flows.

Thank you for highlighting this inaccuracy, we fixed it in our revised manuscript. We also include the Froude number in our analysis and expand the discussion on gravity waves in Appendix C. We update the manuscript as follows:

Line 39: "Gravity waves propagate upstream in their strong free-atmosphere stratification simulation but do not propagate upstream in their weak free-atmosphere stratification simulation (Wu and Porté-Agel, 2017)."

Line 68: "Here, we investigate how atmospheric stability modifies upstream blockage with minimal upstream propagation of gravity waves (see Appendix C for a discussion on gravity waves in our domain)."

Line 490: "We also evaluate the upstream propagation of gravity waves in our simulations using the Froude number, as done by Wu and Porté-Agel (2017). The Froude number characterizes the balance between flow acceleration or deceleration and the pressure gradient imposed by the displacement of the stably stratified flow $Fr = \bar{U} / \sqrt{g'H}$, where \bar{U} is the boundary-layer bulk velocity, $g' = \frac{g\Delta\theta}{\theta_0}$ is the reduced gravity accounting for the inversion strength, and H is the boundary layer height. Wu and Porté-Agel (2017) suggest gravity waves amplify the blockage effect in subcritical flow ($Fr < 1$), where pressure disturbances propagate upstream. The Froude number in our weak and moderate stability simulations is 1.2 and 1.35,

respectively, characteristic of supercritical flow ($Fr > 1$), thus pressure disturbances do not propagate upstream.”

Line 43-45: “Note that Allaerts and Meyers (2017, 2018); Maas (2022) simulate the flow around an infinitely wide wind plant; therefore, the large vertical boundary layer displacement that excites gravity waves (and thus the velocity deceleration in the induction region) is likely overestimated compared to operational wind plants.” This statement is not obvious. Please add a better explanation based on existing literature here.

We include the following for clarification:

Line 42: “Note that Allaerts and Meyers (2017, 2018); Maas (2022) simulate the flow around an infinitely wide wind plant. The power loss due to upstream-propagating gravity waves increases as the wind plant becomes infinitely wide (Allaerts and Meyers, 2019). Therefore, the velocity deceleration in the induction region of an infinitely wide wind plant is likely larger than would be expected in an operational wind plant of finite width.”

On the choice of grid spacing (Line 89-91):

Did the authors carry out any sensitivity tests in order to show that the grid spacing used by them is actually sufficiently fine? If not this should be mentioned in the manuscript.

Because another reviewer also asked about grid resolution, we now include an additional appendix in our manuscript:

Line 494: Appendix D

“Grid resolution in our simulations is sufficient to resolve most turbulence kinetic energy across the turbine rotor layer (Figure D1). For the non-linear backscatter and anisotropy subgrid-scale turbulence model (Kosović, 1997), the total turbulence kinetic energy \bar{k}_{tot} is given as $\bar{k}_{tot} = \frac{1}{2}(\overline{u'_i u'_i} + m_{ii}) + \bar{k}_{SGS}$, where $\overline{u'_i u'_i}$ represents the resolved TKE, m_{ii} are the normal subgrid-scale stress components, and \bar{k}_{SGS} is the subgrid-scale TKE. Nearly 80% of TKE in the turbine rotor layer is resolved by the numerical grid for both simulations (Figure D1). Because less than 80% of TKE in the lower rotor layer is resolved in the weak stability case ($\bar{k}_{res}/\bar{k}_{tot} = 0.78$ at $z = 30$ m), a finer grid is used for the simulation of moderately stably stratified flow.”

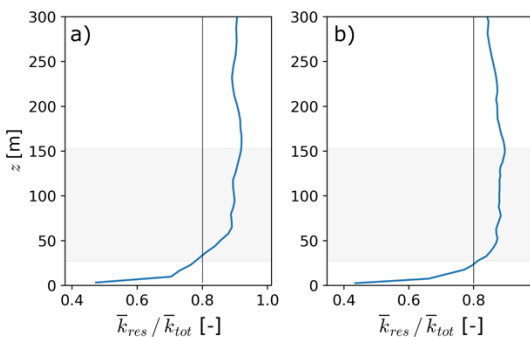


Figure D1: Fraction of resolved TKE in the surface layer for the weak (a) and moderate (b) stability cases. The solid, black line corresponds to 80% of resolved TKE. The grey shaded area corresponds to the turbine rotor layer.

On the choice of the model domain (Figure 1):

Did the authors check whether the 45 D long part of the model domain upstream of the wind farm is actually sufficiently long enough in order to avoid that the inflow boundary has an impact on the blockage that is found in the simulations?

We investigate the effect from prescribed boundary conditions by considering the velocity field close to the domain boundaries. We find that boundary conditions have minimal effects on the flow in both the induction and wake regions. Because the velocity deceleration in the induction region is virtually equal to freestream 30D upstream of the turbines (see Figure 8 below), we conclude that a 45D fetch is adequate to minimize the effects of the upstream boundary condition. At the downstream end of the domain, the wake recovery only appears to be influenced by the boundary conditions very close to the domain boundary.

We add clarification to the text as follows:

Line 107: “As will be shown later in the manuscript, the velocity deceleration in the induction region is virtually zero 30D upstream of the wind plant. Therefore, 45D of fetch upstream of the wind plant is deemed sufficient to investigate the induction region of the turbine array.”

Furthermore, we adjust the x-axis in Figure 8 to show the velocity deceleration far upstream as follows:

Line 183: “The velocity deceleration asymptotes to zero far upstream ($x < -30D$) for both atmospheric conditions (Figure 8).”

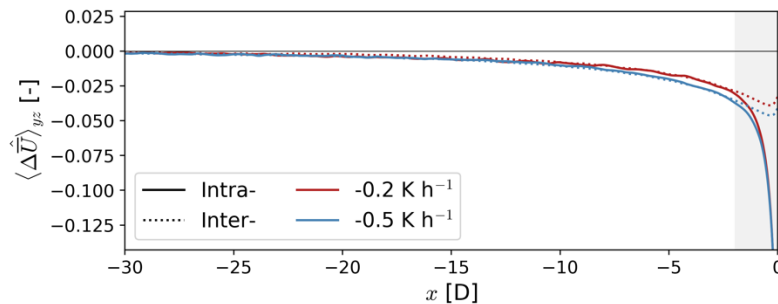


Figure 8: Normalized velocity deficit ($\Delta U = \frac{\bar{U} - \bar{U}_\infty}{\bar{U}_\infty}$) for the inter- and intra-turbine regions upstream of the wind plant for each atmospheric condition...

Did the authors check whether the space in y-direction at the side of the the wind farm is sufficiently large in order to be able to exclude that the simulation results are disturbed by the lateral boundaries? Does the simulation approach the case of an isolated wind farm or that of an infinite wind farm in y-direction?

We acknowledge that the domain size in the streamwise direction can affect blockage. However, we did not perform a sensitivity analysis on the space to the sides of the wind plant because of its high computational costs. We add the following information to the manuscript:

Line 110: "Strickland and Stevens (2022) show the power of front-row turbines in a wind plant is sensitive to the ratio between the wind plant width (L_{y-wp}) and the domain size in the y-direction (L_y). Because the change in turbine power for ratios $L_{y-wp}/L_y < 0.5$ is small (Strickland and Stevens, 2022) but the increase in computational resources is significant, we use a ratio of 0.5 here."

On the set-up of the large-eddy simulations (Section 2.1):

As the geostrophic wind is used as a boundary condition in the simulations, an information on the geographic coordinates where the simulations are carried out should be provided. The geographic coordinates will change the Coriolis parameter and therefore also the profiles of the wind components.

Thank you for pointing this out. We include this information as follows:

Line 127: "Both simulations are initialized with a $U_g = 11$ m/s geostrophic wind speed and the Coriolis parameter is $f_c \approx 9.37 \times 10^{-5}$ 1/s, corresponding to a latitude of 40° ."

On Figure 2:

When is the averaging period that is used in this Figure? Has the simulation reached a stationary state yet?

We add clarification in the caption as follows:

Figure 6: Horizontal wind speed (a), wind direction (b) and potential temperature (c) profiles for the atmospheric conditions simulated herein. Atmospheric variables are averaged spatially over the entire domain and temporally over 1 h after spin-up of turbulence and stability is complete.

On Figure 3:

A line illustrating a function of the type $y=A+k^{(-5/3)}$ (Kolmogorov slope) should be added in order to show that the simulation actually resolves a part of the inertial subrange of turbulence.

We now include this information in the figure. Also, as requested in comments below, we make the colormap consistent in each panel.

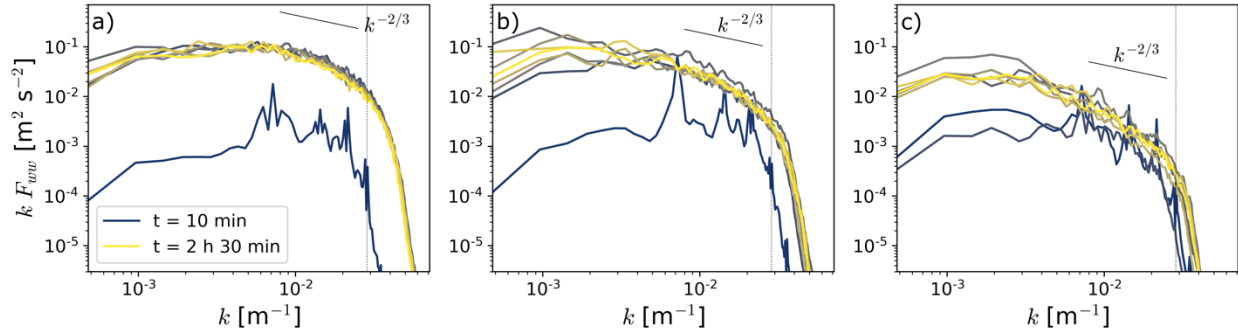


Figure 2: Compensated turbulence spectra of the w -velocity for the $\Delta x = 7\text{m}$ neutrally stratified boundary layer in the precursor simulation at $z=90\text{ m}$ (a), $z=300\text{ m}$ (b), and $z=800\text{ m}$ (c). Colored lines indicate time since initialization in 20-minute time increments. The dotted, black vertical line in each plot represents the effective grid resolution ($4\text{--}5 \Delta x$) expected from the reduced advection scheme in our simulations (Kosović et al., 2016). The theoretical $-2/3$ Kolmogorov slope for the inertial range is indicated by the solid black line in each plot.

On Figure 5:

The Figure shows clearly an inertial oscillation that is triggered when the cooling of the atmospheric boundary layer starts. Obviously, the inertial oscillation has not been completely damped after 8 h. What does this mean for the analysis of the global blockage effect?

We acknowledge that the stable boundary layer is still evolving, and this is expected because of the cooling rate at the surface. However, the effect from this boundary layer evolution is minimal over the simulation time (1 h). As shown in the shaded areas in Figure iii, the change in hub-height wind direction, a proxy for the inertial oscillation, over the simulation period (1 h) is smaller than 1 degree.

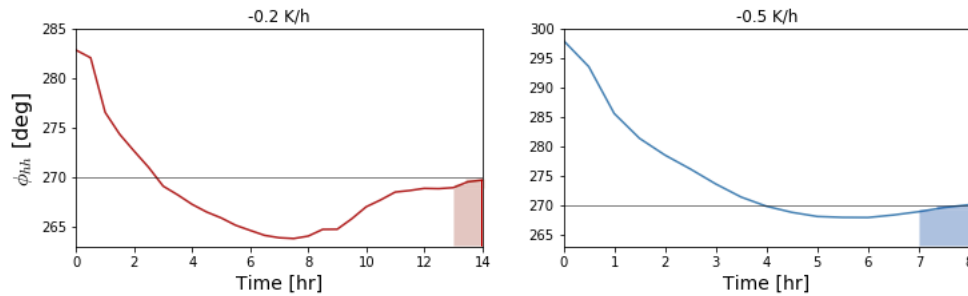


Figure iii: Time series of hub-height wind direction for each atmospheric condition over the simulation period. The shaded area in each plot represents the simulation time period for evaluating blockage.

We include the following in the manuscript:

Line 168: “Over the simulation period, hub-height wind direction varies by less than 1° for both atmospheric conditions.”

We also direct the reviewer to the discussion of the physical mechanisms modifying blockage where we discuss the effect of Coriolis forcing, which drives the inertial oscillation:

Line 212: “Even though the Coriolis force in our simulation domain is not negligible, Coriolis forcing in the induction region is small. The Coriolis parameter scales as $f_c \sim 10^{-4} \text{ s}^{-1}$ and the v -velocity in the turbine rotor layer for both stability cases is on the order of $\bar{v} \sim 0.1 \text{ m/s}$, thus Coriolis forcing is of the order $f_c \bar{v} \sim 10^{-5} \text{ m/s}^2$.”

On Figure 6:

It is difficult to show with Figure 6 that the Monin-Obukhov-length and the Richardson number have already reached stationary values within the simulation time used (even for the case with the stronger cooling rate).

We don't expect the stability metrics in our simulations to reach a steady state because we have a cooling rate at the surface, which is anticipated to result in a continual evolution of the boundary layer. We provide clarification in the text as follows:

Line 155: “The -0.5 K/h simulation is run until the temporal change in bulk Richardson number in the surface layer and the Obukhov length is small.”

Line 162: “Note that we do not expect our simulations to reach a steady state because the cooling rate at the surface continually modifies stability in the surface layer. Nonetheless, the evolution of the surface layer is slow after 8 h (13 h) for the moderate (weak) stability simulation.”

Line 201:

When reading the manuscript I understood that independent of the simulation each differential control volume has an extension of 15 m along the x-direction. However, how does this work out when the grid spacing is 7 m in one of the two cases simulated?

Thank you for catching this, we interpolate both numerical grids to a common grid with horizontal spacing equal to 15 m, which is close to a common multiple of both grid resolutions. We tested different common grids, but there were no appreciable differences in the results. We clarify this in the manuscript:

Line 222: “Because grid spacing is different for the stability cases, we interpolate atmospheric variables from each simulation to a common grid with horizontal resolution of 15 m.”

Figure 11:

The authors should elaborate a bit more on the explanation of the observation that the decrease of pressure starts already slightly upstream of the actuator disk.

The maximum in the pressure perturbation field upstream of the turbine is located slightly upstream of the GAD model. The maximum in the pressure field upstream of the turbines has been reported in the literature (e.g., Figure 12 in Strickland and Stevens, 2022).

We add the following Figure and clarification to the text:

Line 235: “The thrust force imparted by the turbine to the flow is a fundamental driver for blockage (Ebenhoch et al., 2017). In the numerical implementation of the GAD model, the aerodynamic forces are spread across multiple grid cells along the streamwise direction to avoid numerical instabilities (Mirocha et al., 2014). A pressure gradient upstream of the turbine forms in response to the thrust force that the turbine imparts on the flow ($\Delta\bar{p}_{pert}/\Delta x > 0$ upstream of the turbine in Figure 12). Because the thrust force is spread across multiple grid cells in the streamwise direction, the maximum in pressure in front of the turbines is located slightly upstream of the actual location of the GAD in the numerical domain (Figure 12). As a result, we restrict the control volume V in Figure 11 to extend up to $x=5647$ m, the location of the maximum in pressure perturbation upstream of the turbine array (vertical dotted line in Figure 12).”

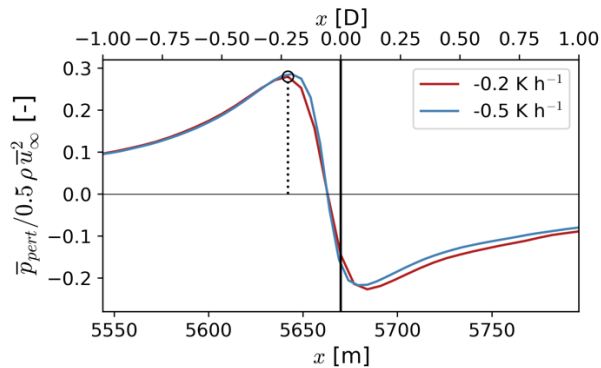


Figure 12: Hub-height pressure perturbation of a front-row turbine in the wind plant for each stability case. The pressure perturbation is normalized over the corresponding dynamic pressure for each stability condition. The solid black vertical line illustrates the location of the GAD in the numerical domain. The dotted vertical line illustrates the local maximum in pressure perturbation upstream of a front-row turbine in the wind plant. The secondary x-axis is scaled to locate $x=0D$ at the location of the front-row turbine.

Line 246: “Immediately upstream of the turbine (cross-hatched area in Figure 13), the pressure gradient force becomes negative because the GAD produces a pressure drop in the flow and the pressure perturbation field reaches a local maximum slightly upstream of the turbine (Figure 12). In the numerical implementation of the GAD model, the aerodynamic forces are spread across multiple grid cells to avoid numerical instabilities (Mirocha et al., 2014), which causes the pressure field to decrease over multiple grid cells (Figure 12).”

We also modify the relevant figures in the manuscript (Figures 13, 14, 16, 17, 18, 19, 20) to highlight this pressure drop that happens across the grid cells that intersect the GAD. An example is Figure 13 in the manuscript:

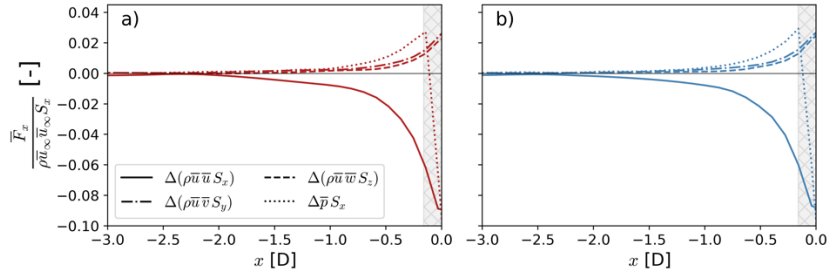


Figure 13: Streamwise evolution of the u-momentum equation (Eq. 2) for a stand-alone turbine in the weak (a) and moderate (b) stability cases. The integral momentum equation is evaluated on differential control volumes δV along the x-direction, as shown in Figure 11. The x-axis is scaled to locate $x=0D$ at the location of the turbine. The mean momentum fluxes and the pressure gradient force are normalized using the u-momentum flux at the inflow of the control volume far upstream ($\rho\bar{u}_\infty\bar{u}_\infty S_x$) for the respective stability case. The cross-hatched area in each panel illustrates the grid cells influenced by the thrust force from the GAD.

We also add clarification in the text as follows:

Line 255: “Note that the momentum balance immediately upstream of the turbine (cross-hatched area in Figure 13) is not equal to zero because the thrust force from the GAD is not included in our calculations.”

Figure B1:

This is one of the main findings and should be integrated in the results part of the manuscript.

Please see comment above, where we clarify that the primary cause for an increase in vertical advection of u-momentum is larger shear of the vertical velocity ($\frac{\Delta\bar{u}}{\Delta z}$) within the turbine rotor layer.

General and technical comments

- Whole document: Use non-italic units, introduce a Space between number and unit, avoid line breaks between number and unit, add clickable links in the pdf for references on figures etc.

We appreciate this suggestion. We use non-italic units throughout the text, include a space in between the number and unit, and add clickable links throughout the pdf.

- Line 17: Please add a reference for wind turbine and cluster wakes each.

We update the text as follows:

Line 19: “Wind turbine and wind plant wakes can also affect power production of downstream turbines (El-Asha et al., 2017) and plants (Stieren and Stevens, 2022), an effect known as wake loss.”

- Line 18-19: Why are so many references given here? One reference with a more general view on blockage like Bleeg et al., 2018 is sufficient, the others will be addressed in the state of the art.

Thank you for your suggestion, we modify the manuscript to only include reference to Bleeg et. al (2018).

- Line 21: “know” needs to be replaced by “known”

We modify the manuscript accordingly.

- Line 29-30: Please sort relevant references to the named factors influencing global blockage (“size and layout of the wind plant, atmospheric conditions, wind turbine characteristics, and wind speed”)

As requested by the reviewer, we sort the references as follows:

Line 27: “The velocity deceleration within the induction region can vary substantially depending on the size and layout of the wind plant (e.g., Centurelli et al., 2021; Strickland and Stevens, 2022; Strickland et al., 2022; Bleeg et al., 2018), atmospheric conditions (e.g., Allaerts and Meyers, 2018, 2017; Bleeg and Montavon, 2022; Schneemann et al., 2020; Strickland et al., 2022), wind turbine characteristics (e.g., Ebenhoch et al., 2017), and wind speed (e.g., Schneemann et al., 2020).”

- Line 33-35: The named references show different velocity deficits in different distances upstream. Please specify the general statement here.

Thank you for your suggestion. We considered including a more detailed description of the velocity deceleration from each study. However, the objective of this paragraph is to highlight the order-of-magnitude difference in the velocity deficit reported in some studies, rather than the velocity deceleration from each research paper. Therefore, we consider that providing a general statement is more valuable to the reader than giving detailed information about each reference.

- Line 62: “neutral LES” This is uncommon terminology. Please change to e.g. “The authors simulated a neutrally stratified boundary layer flow using LES...”

Line 63 now reads: “Using LES of neutrally stratified boundary-layer flow, Strickland and Stevens (2022) show an increase in the adverse pressure gradient upstream of wind plants with closely-spaced turbines in the cross-stream direction.”

We also update the captions of Figures 2 and 3 to replace “neutral LES” with “neutrally stratified boundary layer”.

- Line 89: The terminology introduced here for the state of the atmosphere should be kept throughout the document. The authors simulate a weakly stable boundary layer and a moderately stable boundary layer. Changing this to “moderately and weakly stratified flow” without referring to “stable” is misleading.

Thank you for your suggestion. We update the manuscript so that we always refer to stably stratified flow, following the convention found in the literature (e.g., Allaerts and Meyers, 2018). For example, Line 349 now reads: “The wind speed is 3.5% and 2.8% slower than freestream 2D upstream of the wind plant for moderately and weakly stably stratified flow.”

- Figure 1: Please add the turbine spacing in x and y direction in the Figure or the caption.

We update the caption in Figure 1 as follows:

Figure 1: Relative location of the turbines in the wind plant (a) and stand-alone turbine (b) simulations for evaluating blockage. Forty NREL 5MW wind turbines constitute the 200MW wind plant simulated herein. Turbine spacing is 7D and 3.5D in the streamwise and cross-stream directions, respectively.

- Table 1: Please add information about the stability, i.e. the cooling rate applied.

We updated Table 1 in the manuscript to include the cooling rate at the surface for each stability condition.

- Line 113: Adding the word “temporal” makes the method more clear here: ... we prescribe a temporal cooling rate rather than...

We add the word “temporal” as suggested. Line 121 now reads: “... we prescribe a temporal cooling rate rather than a heat flux at the surface.”

- Line 113: flow -> flows are...

We modify the manuscript accordingly.

- Figure 2: Please label the height axis as z. Please add information about the period the data is averaged on. How long was the cooling applied before the averaging period? Further, Figure 2 shows the resulting profiles while Figure 3 and 4 jump back to the pre run simulations. This is a bit confusing while reading and should be restructured.

Thank you for your suggestions. We replace the “Height” label with “z” throughout the manuscript (Figures 3, 4, 6, A2, A4, D1). We move the figure showing the final atmospheric conditions to the end of section 2.2 so that it appears after we describe spin-up for our simulations. We also update the caption to include information about the temporal averaging as follows:

Line 165: “Atmospheric conditions after spin-up of turbulence and stability are shown in Figure 6.”

Figure 6: Horizontal wind speed (a), wind direction and potential temperature (c) profiles for the atmospheric conditions simulated herein. Atmospheric variables are averaged spatially over the entire domain and temporally over 1 h after spin-up is complete.

- Figure 3: The legend just holds two entries while the Figure includes many different curves / colors. The colours seem not to be consistent through the subplots. The evolution is hard to

follow and the description from Line 126 ff could not be reproduced. Please change the legend or introduce a colour scale. In my opinion the amount of curves shown can and should be reduced. Further, please add the Kolmogorov slope into the plots. Please state in the caption that this is a plot of a pre-run of the LES.

We appreciate your suggestions to make this figure clearer. We modify the figure so that the colormap is consistent across the different panels. We also reduce the number of curves shown in half and include the theoretical Kolmogorov slope. We update the caption to clarify that these results are for the precursor neutral LES.

Figure 2: Compensated turbulence spectra of the w -velocity for the $\Delta x = 7\text{m}$ neutrally stratified boundary layer in the precursor simulation at $z=90\text{ m}$ (a), $z=300\text{ m}$ (b), and $z=800\text{ m}$ (c). Colored lines indicate time since initialization in 20-minute time increments. The dotted, black vertical line in each plot represents the effective grid resolution ($4\text{-}5 \Delta x$) expected from the reduced advection scheme in our simulations (Kosović et al., 2016). The theoretical $-2/3$ Kolmogorov slope for the inertial range is indicated by the solid black line in each plot.

- Figure 4: z for height axis, readable legend covering all cases as for Figure 3. Maybe Figure 3 and 4 can be even combined.

We incorporated your suggestions in the text. As described above, we changed the label for the y -axis to “ z ”. Also, like in the previous comment, we reduce the number of curves and update the caption to clarify that these results are for the precursor neutral LES and that the colored lines correspond to different times since the simulation is initialized. We decided not to combine Figures 2 and 3 because one relates to turbulence development and the other to the mean flow.

Figure 3: Vertical profile of the horizontal wind speed for the $\Delta x = 7\text{ m}$ neutrally stratified boundary layer. The velocity profile is averaged spatially over the entire domain. Colored lines indicate time since initialization in 20-minute time increments.

- Caption Figure 4: “Horizontal velocity profile” is misleading, e.g. “vertical profile of the horizontal wind” is more clear.

We clarify the caption of Figure 3 as shown in the comment above.

- Line 131: Delete “On average”, the information is double.

We modify the manuscript accordingly.

- Line 149: “Nose” is a not common expression for the wind speed maximum of a LLJ. Please use a more common expression.

We appreciate your suggestion, however the atmospheric science literature commonly refers to wind speed maximum of the low-level jet as the nose (e.g., Banta et al., 2002; Vanderwende et al., 2015; Carroll et al., 2019; Brogno et al., 2021; Smith et al., 2019).

- Figure 6: Where is the benefit in showing both L and Ri_{bulk} ? Further, both cases seem not to have converged. Please elaborate on this.

As we mention in the comments above, we don’t expect the stability metrics in our simulations to reach a steady state because we have a cooling rate at the surface, which is expected to

result in a continual evolution of the boundary layer. We see value in showing both stability parameters because L describes stability at the surface whereas Ri describes stability across the turbine rotor layer, both of which are important in our simulations. We provide clarification in the text as follows:

Line 155: “The -0.5 K/h simulation is run until the temporal change in bulk Richardson number in the surface layer and the Obukhov length is small.”

Line 162: “Note that we do not expect our simulations to reach a steady state because the cooling rate at the surface continually modifies stability in the surface layer. Nonetheless, the evolution of the surface layer is slow after 8 h (13 h) for the moderate (weak) stability simulation.”

- Line 155: Better use $^{\circ}$ instead of deg in the whole document.

Thank you for your suggestion, we modify the manuscript and figures accordingly.

- Figure 7: A second x-axis in units of D could support readability. Within the stippled areas the wind field cannot be well seen. We suggest to remove the stipples and just keep the bordering lines and labels. Why is the wake region marked as well?

Thank you for your suggestion. We considered removing the stippled areas; however, the only reason for this figure is to clearly define the inter- and intra-turbine regions, and the stippled areas are very effective in doing so. Therefore, we decide to leave them in the figure. Nonetheless, we update the figure so that the stippled areas only cover the induction region of the turbines and not the wakes.

- Figure 9: Caption could refer to Figure 8 saving copy/pasted information. Even better could be to combine both plots as subplots in a single Figure. Same could be applied for some of the following results plots.

As pointed out in the Community Comment (CC1), we had a typo on the caption. We updated the caption to emphasize that the velocity deficit is averaged in the y-direction over the intra-turbine region, which corresponds to the stippled area in Figure 7.

- Line 192, Equation 1: Labelling of the different terms can help the reader to follow more easily.

Thank you for your suggestion, we include labelling in Equation 1 and Equation B1.

- Line 224ff: The small differences described could not be seen in the Figure. At which position does the difference occur?

We clarify as follows:

Line 259: “In the entire control volume V in Figure 11d, the pressure gradient force that drives flow deceleration upstream of the turbine differs by 3.1% between atmospheric conditions.”

- Line 254: “atmospheric” needs to be changed to atmospheric

We modify the manuscript accordingly.

- Line 259: Please elaborate a bit more on the mentioned secondary circulation as it is not obvious to the reader.

We find that the change in u-velocity is transformed into a change in w-velocity. Also, as requested by another reviewer, we clarify the manuscript and replace “secondary circulation” with “secondary flow feature” as follows:

Line 293: “Mass balance indicates the slowdown of the u-velocity in the turbine rotor layer ($\Delta(\rho\bar{u}S_x) < 0$) is balanced by the development of a secondary flow feature in the form of net-upwards vertical motion ($\Delta(\rho\bar{w}S_z) > 0$) for both stability conditions (i.e., $\Delta(\rho\bar{u}S_x) + \Delta(\rho\bar{w}S_z) \approx 0$).”

- Line 260: “ The increase in vertical velocity is driven by a vertical pressure gradient...” What is the driver for this pressure gradient? This seems to be one of the most relevant findings, please better explain and highlight.

We direct the reviewer to the comments above, where we show that the primary amplifier for blockage is vertical shear of the horizontal velocity over the turbine rotor layer. We also want to stress that the idea of the vertical momentum analysis is to show that vertical motions can form in stably stratified flow, even though there is a downward buoyancy force. We clarify as follows:

Line 296: “The development of the vertical velocity is possible because of a vertical pressure gradient that balances the downward buoyancy force in the stably stratified flow (see Appendix B for a deeper analysis on vertical momentum balance).”

- Line 287: please change “x1.9” to 1.9 times

We modify the manuscript accordingly.

- Line 291-292: Bleeg et al. (2018) suggest (plural)

We modify the manuscript accordingly.

- Line 332-343: Please elaborate more on the difference between momentum advection and a deflection of momentum upwards. This is not obvious.

We direct the reviewer to Line 341 in the revised manuscript, where we elaborate on momentum advection and flow deflection as follows:

Line 344: “The slowdown of the u-velocity in the induction region of the wind plant is transferred into vertical motions (Figure 18). Other simulation studies have also noted this vertical deflection of the flow (e.g., Wu and Porté-Agel, 2017; Allaerts and Meyers, 2017). The vertical velocity advects horizontal momentum out of the turbine rotor layer.”

We also add clarification as follows:

Line 382: "... they suggest an increased pressure gradient amplifies blockage as cold air is deflected upwards (i.e., u-velocity is transformed into w-velocity)."

Literature

Allaerts, D. and Meyers, J.: Boundary-layer development and gravity waves in conventionally neutral wind farms, *Journal of Fluid Mechanics*, 814, 95–130, <https://doi.org/10.1017/jfm.2017.11>, 2017.

Allaerts, D. and Meyers, J.: Gravity Waves and Wind-Farm Efficiency in Neutral and Stable Conditions, *Boundary-Layer Meteorology*, 166, 269–299, <https://doi.org/10.1007/s10546-017-0307-5>, 2018.

Bleeg, J., Purcell, M., Ruisi, R., and Traiger, E.: Wind Farm Blockage and the Consequences of Neglecting Its Impact on Energy Production, *Energies*, 11, 1609, <https://doi.org/10.3390/en11061609>, 2018.

Maas, O.: From gigawatt to multi-gigawatt wind farms: wake effects, energy budgets and inertial gravity waves investigated by large-eddy simulations, <https://doi.org/10.5194/wes-2022-63>, 2022.

Schneemann, J., Theuer, F., Rott, A., Dörenkämper, M., and Kühn, M.: Offshore wind farm global blockage measured with scanning lidar, *Wind Energy Science*, 6, 521–538, <https://doi.org/10.5194/wes-6-521-2021>, 2021.

Strickland, J. M. and Stevens, R. J.: Investigating wind farm blockage in a neutral boundary layer using large-eddy simulations, *European Journal of Mechanics - B/Fluids*, 95, 303–314, <https://doi.org/10.1016/j.euromechflu.2022.05.004>, 2022.

Wu, K. and Porté-Agel, F.: Flow Adjustment Inside and Around Large Finite-Size Wind Farms, *Energies*, 10, 2164, <https://doi.org/10.3390/en10122164>, 2017.